## **Supplementary Figure Legends**

Supplementary Figure 1. Binding of the cochlin mutants to various glycans. Binding was examined by evanescent-field fluorescence detection using a microarray containing 16 monosaccharides, 59 oligosaccharides including six GAGs, HA, chondroitin sulfate A (CSA), dermatan sulfate (also called CSB), heparan sulfate (HS), heparin (HP), and keratan sulfate (KS), and 21 glycoproteins [24]. Sulfated oligosaccharides and sulfated glycosaminoglycans are highlighted in yellow. Mouse cochlin(FL)-Fc specifically bound to heparin and did not bind to any other spots. Values represent mean ± standard deviation (n = 2).

Supplementary Figure 2. Inhibition assay of cochlin-Fc binding to immobilized heparin by several GAGs. Mouse cochlin(FL)-Fc was preincubated with the indicated concentration of GAG for 1 h at 20  $^{\circ}$ C and then measured the binding of cochlin-Fc to immobilized heparin was performed. Values represent mean  $\pm$  standard deviation (n = 3). DS, CSC, CSD showed like that of CSA.

Supplementary Figure 3. The expressed region of truncated mutants Eight truncation mutants of mouse cochlin were designed and prepared to investigate regions

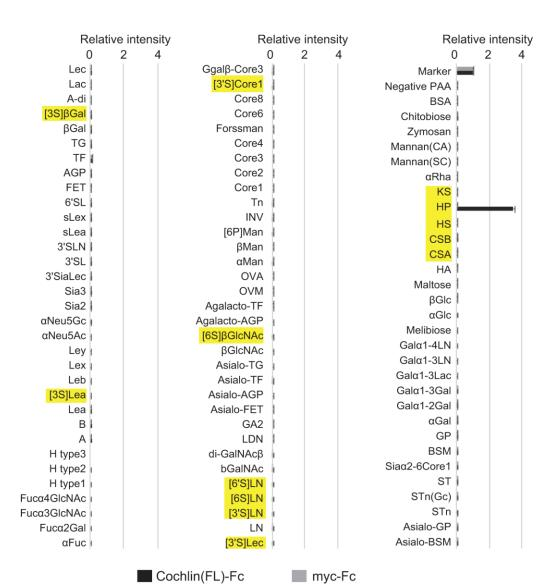
that contribute to GAG recognition. The residues expressed for truncation mutants were determined based on the results of the secondary structure prediction by PSIPRED (http://bioinf.cs.ucl.ac.uk/psipred/). The amino acid sequence of basic amino acid-rich region between the LCCL and vWA1 domains (from K149 to K161) has been described.

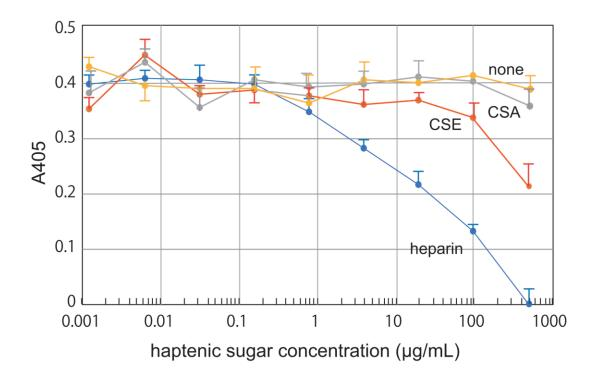
Supplementary Figure 4. GAG-binding specificities of cochlin-Fc mutants. The binding activity of each cochlin mutant fused to human IgG-Fc ( $\Delta$ LCCL\_b; residues 153–552, LCCL\_a; residues 27–130, LCCL\_b; residues 27–153, LCCL\_c residues 27–158 or vWA2; residues 355–552) was examined by indirect ELISA. Biotinylated GAGs were immobilized on streptavidin-coated microtiter plates and cochlin mutants were added to the wells at a concentration of 1.5  $\mu$ g/mL. Values represent mean  $\pm$  standard deviation (n = 2).

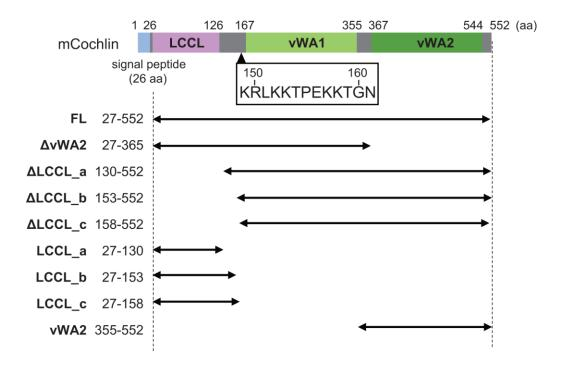
**Supplementary Figure 5. Schematic illustration of the mechanism by which cochlin recognizes several GAGs.** It was suggested that the vWA1 domain was essential for the binding of cochlin to GAGs, and the vWA2 domain and the loop region between the LCCL and vWA1 domains were involved in the interaction. The loop region specifically recognizes highly sulfated GAGs by cochlin (FL) in a coordinated manner.

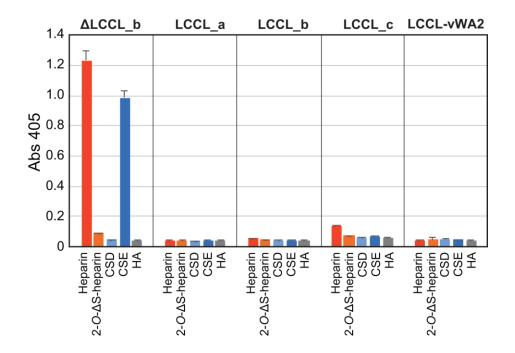
GAG-binding specificity broadened when cochlin lacked the vWA2 domain ( $\Delta$ vWA2). An LCCL-truncation mutant of cochlin ( $\Delta$ LCCL\_a) showed highly specific binding to heparin and CSE.

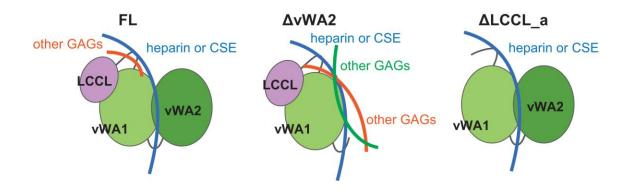
Supplementary Figure 6. Electrostatic surface potential mapped on a homology model of vWA1 and vWA2 domains of mouse cochlin. The 3-dimensional homology model was predicted by SWISS-MODEL (https://swissmodel.expasy.org/interactive) using the structural information of PTMP1 (PDBID: 4CN9), which was predicted as the optimal model. The electrostatic surface potential, calculated using APBS (https://www.poissonboltzmann.org), was visualized using CueMol (http://www.cuemol.org). Positively and negatively charged surfaces are colored in blue and red, respectively.

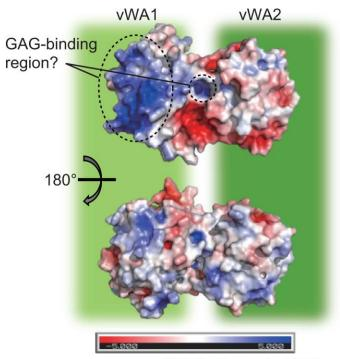












PDB ID of template: 4CN9